

# Processing, Structure, and Mechanical Properties of As-Spun Polypropylene Filaments—A Systematic Approach Using Factorial Design and Statistical Analysis

Ruodan Yang, Robert R. Mather, Alex F. Fotheringham

Biomedical Textiles Research Centre, School of Textiles and Design, Heriot-Watt University, Netherdale, Galashiels, TD1 3HF, Scotland

Received 1 April 2004; accepted 15 August 2004

DOI 10.1002/app.21416

Published online 26 January 2005 in Wiley InterScience (www.interscience.wiley.com).

**ABSTRACT:** Polypropylene filaments spun under a factorial experimental design were characterized with respect to filament tenacity, elongation, and specific secant modulus. These quantities were assessed quantitatively as responses to seven selected processing parameters using standard statistical methods. It was found that among all the significant factors identified, the draw-down ratio, which combines metering pump speed (MPS) and filament winding speed (WS), exerts the most significant effects on all the three responses. The grade of polypropylene used, as denoted by its melt flow index (MFI), also significantly influences tenacity and modulus. Spinning temperature, too, influences modulus. In addition, the significant influence of two interaction effects, MPS\*WS and MFI\*WS, is demonstrated. A

further feature of the study is systematic correlation of physical properties with microscopic structure as well as processing conditions. The study has demonstrated that the statistical approach to the development of fiber process technology has the advantages of a one-step overall design, considerably reduced experimental size, and systematic analysis leading to concise models with known levels of confidence. © 2005 Wiley Periodicals, Inc. *J Appl Polym Sci* 96: 144–154, 2005

**Key words:** statistical analysis; factorial experimental design; filament mechanical properties; filament structural properties; polypropylene

## INTRODUCTION

World-wide production of polypropylene (PP) fibers has increased by more than five times since 1980, considerably surpassing that of polyamide and acrylic fibers.<sup>1,2</sup> This outstanding success can be attributed to the prominent advantages of this versatile material, and hence to its rapid expansion into more diverse applications. PP fibers possess good resistance to chemicals, good stain and abrasion resistance, low density, low thermal conductivity, low moisture absorption, and excellent toughness and resilience.<sup>3</sup> Some of these features are advantageous for domestic use, such as stain and abrasion resistance for home furnishing and upholstery fabrics, and lightweight and thermal insulation for comfort and warmth of clothing fabrics. The combination of abrasion resistance, stain resistance, and high resilience is desirable for carpet materials. Other features beneficial for technical use are good chemical resistance for finishing processing, toughness for reinforcement of paper, plastic, and cement, and a combination of high strength (wet and dry), light weight, low moisture absorption, and resistance to abrasion for rope mate-

rials.<sup>3</sup> Recently, the use of PP fibers has been expanded to new areas, such as nonwoven fabrics for medical and hygiene applications. Development of desired properties and expansion of applications has been achieved in some cases mainly through new polymerization techniques and new additives. In other cases, the development of desired properties has been achieved principally through improvement of processing technology.<sup>4</sup> In all circumstances, processing plays a critically important role in the development of end-use fiber products.

Fiber processing normally involves multiple parameters and their interactions. However, the approach of “one factor at a time” to the development of processing technology can be time consuming and costly. In this “traditional” approach, only one factor is changed at a time while other factors are kept constant. As a result, a large number of experiments are necessarily required. Furthermore, interaction effects between individual parameters cannot be readily studied, thus often giving an incorrect model of the process of interest. Recently, a statistical approach comprising factorial experimental design and comprehensive statistical analysis has been applied to studies of PP fiber processing.<sup>5–9</sup> In contrast to the traditional approach, the statistical approach identifies both interaction effects and individual factor effects. Therefore, more accurate and reliable conclusions in relation to the process can be reached.

Correspondence to: R. Mather (R.R.Mather@hw.ac.uk).

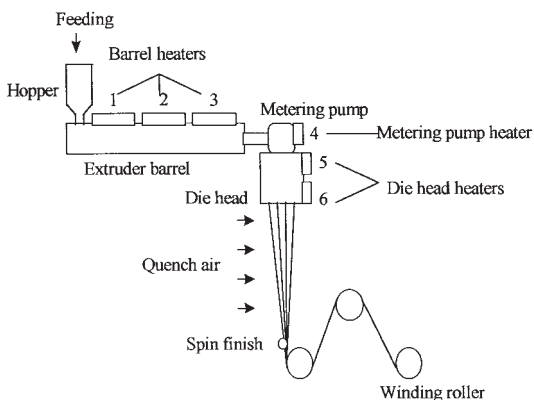


**Figure 1** Schematic diagram for the melt spinning of PP fibers. The numbers refer to heaters in the melt spinning equipment.

This article concentrates on our work on the application of the statistical approach to the investigation of the factors controlling mechanical properties of the as-spun PP filament, including tenacity, elongation to break, and specific secant modulus. Specific secant modulus, determined over the 2–5% range of filament elongation, is often more reliably determined than initial modulus, evaluated from the initial slope of a stress-strain curve for a filament. The results of the investigation of factors controlling structural properties, including crystallographic order (assessed from the reciprocal of the half-height width of the 110 plane in a wide-angle X-ray diffraction pattern<sup>10</sup>) and overall orientation of molecular chains, using the same approach, have been reported in a previous article.<sup>11</sup> The mechanical characteristics, analyzed in this paper by standard statistical methods,<sup>12–15</sup> are correlated with the structural features. The overall aim is to establish a more systematic understanding of the processing-structure-properties relationship in PP filaments and, thus, more efficient development of process technology.

## EXPERIMENTAL TRIALS

The melt spinning of raw PP granules was carried out on a melt extrusion machine<sup>6,11</sup> from Extrusion Systems Limited (ESL), illustrated schematically in Figure

1. From the granules to as-spun filaments, the raw PP materials went through extruding and melting in the extruder; metering by the metering pump; filtering and orientated flow through the die head (with a filter package and a spinneret of 55 circular holes); air quenching by ambient, side-blow air; spin finish application; and winding. The change in spinning temperature was effected by adjusting the heaters on the metering pump and the die head (heaters 4, 5, and 6 in Fig. 1.).

The experiments involved seven control factors that covered the significant variables in spinning processing:<sup>6,11</sup> grades of PP (represented by the melt flow index, MFI), spinning temperature (ST), metering pump speed (MPS), hole size of spinneret (HS), quenching air speed (QAS), application speed of spin finish (SFS<sub>s</sub>), and winding speed (WS). Two levels were used for each factor, as shown in Table I. To expand design space, the two levels were separated as far apart from one another as was practically feasible. The two grades of PP raw material used were PPH9069 (Finapro) and VC18 (Borealis), with MFI values of 22.4 (±0.2) and 17.7 (±0.2) g/10 min, respectively.

An L16 fractional factorial experimental design<sup>12</sup> was employed. The detailed experimental arrangement of the sixteen trials is shown in Table II. Also shown in Table II are values for the draw-down ratio (DDR), the ratio by which the filaments have been stretched during their passage from the spinneret to the winder. The sixteen trials were randomly conducted over two consecutive days, with a block of eight trials for each day. The entire trial set was duplicated in a different random order. In addition, a set of confirmatory trials (shown in Table III) was conducted, to test the correctness of the model and to evaluate the significance of interactions between control parameters. In this third series of trials, QAS and SFS<sub>s</sub> were omitted, as discussed below.

Tensile testing was carried out in a conditioned atmosphere with a temperature of (20 ± 2)°C and a relative humidity of (65 ± 3)%. Filaments with initial length 20 mm were stretched at a constant cross-head speed, 20 mm min<sup>-1</sup>. Fiber tenacity (specific stress at break), specific secant modulus, and elon-

**TABLE I**  
Melt Spinning Parameters and Their Levels

Parameters	Abbreviation	Low level	High level
Material melt flow index, g/10 min	MFI	17.7	22.4
Spinning temperature, °C	ST	230	260
Metering pump speed, rpm	MPS	3	12
Spinneret hole size, mm	HS	0.35	0.40
Quench air speed, %	QAS	30	50
Application speed of spin finish, rpm	SFS	0.35	0.50
Winding speed, m min <sup>-1</sup>	WS	100	400

**TABLE II**  
Experimental Array and Average Responses\*

Std. no.	HS mm	WFI g/10 min	ST °C	MPS rpm	QAS %	SFS rpm	WS m min <sup>-1</sup>	DDR	SST		Tenacity cN tex <sup>-1</sup>		Elongation %		Modulus cN tex <sup>-1</sup>	
									(a)	(b)	(a)	(b)	(a)	(b)	(a)	(b)
1	0.35	17.7	230	3	30	0.35	100	111	B B	11.7 (0.3)	8.8 (0.8)	736 (34)	684 (10)	16.7 (2.1)	19.5 (1.4)	
2	0.35	17.7	230	12	30	0.50	400	114	B B	13.9 (0.4)	10.2 (0.4)	580 (17)	546 (5)	22.9 (2.5)	21.1 (0.9)	
3	0.35	17.7	260	3	50	0.35	400	444	A A	29.5 (0.9)	17.2 (0.7)	313 (26)	298 (4)	45.6 (3.9)	33.9 (3.0)	
4	0.35	17.7	260	12	50	0.50	100	29	C C	5.4 (0.2)	5.7 (0.5)	1790 (49)	1686 (12)	16.7 (2.0)	14.6 (1.2)	
5	0.35	22.4	230	3	50	0.50	100	111	B B	9.0 (0.4)	8.1 (0.5)	702 (16)	656 (8)	32.0 (3.1)	27.8 (2.4)	
6	0.35	22.4	230	12	50	0.35	400	114	B B	10.4 (0.4)	9.6 (0.3)	636 (45)	653 (9)	44.6 (2.7)	33.7 (1.8)	
7	0.35	22.4	260	3	30	0.50	400	444	A A	15.1 (0.5)	14.1 (0.2)	463 (19)	550 (9)	50.6 (2.0)	42.4 (1.7)	
8	0.35	22.4	260	12	30	0.35	100	29	C C	6.3 (0.8)	6.1 (0.3)	1672 (61)	1508 (10)	21.8 (1.7)	21.0 (1.9)	
9	0.40	17.7	230	3	50	0.50	400	571	A A	22.8 (0.9)	16.2 (0.4)	318 (16)	428 (10)	63.5 (1.9)	46.3 (2.3)	
10	0.40	17.7	230	12	50	0.35	100	37	C C	6.4 (0.3)	6.1 (0.3)	1560 (66)	1480 (25)	17.9 (1.5)	17.2 (1.3)	
11	0.40	17.7	260	3	30	0.50	100	143	B B	8.4 (0.3)	8.2 (0.3)	1084 (16)	1004 (8)	16.1 (3.4)	14.2 (1.4)	
12	0.40	17.7	260	12	30	0.35	400	148	B B	13.1 (0.1)	10.7 (0.4)	716 (37)	760 (16)	21.7 (1.4)	18.8 (1.3)	
13	0.40	22.4	230	3	30	0.35	400	571	A A	15.5 (0.4)	13.5 (0.9)	532 (37)	626 (5)	63.2 (3.0)	47.7 (1.7)	
14	0.40	22.4	230	12	30	0.50	100	37	C C	7.2 (0.6)	6.3 (0.2)	1700 (63)	1518 (22)	26.9 (1.4)	24.4 (1.4)	
15	0.40	22.4	260	3	50	0.35	100	143	B B	9.0 (0.6)	8.1 (0.1)	830 (40)	874 (22)	20.0 (1.4)	17.4 (0.7)	
16	0.40	22.4	260	12	50	0.50	400	148	B B	9.9 (0.3)	9.5 (0.3)	692 (23)	710 (13)	32.0 (1.3)	28.4 (0.9)	

\* See Table I for the abbreviations of the control factors. DDR represents draw-down ratio, and SST stress-strain type. Columns (a) are for the original series and (b) the duplicate series. The data in brackets are the standard deviation of five repeated measurements.

gation to break were measured using an M5 NENE tensile tester. Five measurements were made for each sample.

The determination of the wide-angle X-ray diffraction and optical birefringence data has been reported elsewhere.<sup>6,11</sup>

**METHODS OF STATISTICAL ANALYSIS**

The principal methods of statistical analysis utilized were main effects plots, analysis of variance

(ANOVA), and interaction plots. The ANOVA was conducted using "MINITAB" software. The main effects reveal the relative magnitude and direction of the effects of individual process control parameters.<sup>14</sup> The ANOVA provides a quantitative index, the F-value, for judging the significance of factor effects, within a chosen level of risk,  $\alpha$ . In accordance with common practice, a level of risk,  $\alpha = 0.05$ , has been used in our work. From the F-value, the probability, P, of the significance of each effect is determined and compared with  $\alpha$ .

**TABLE III**  
Experimental Array and Tensile Data for As-Spun PP Filaments Obtained from the Third Series\*

Std. no.	HS mm	WFI g/10 min	ST °C	MPS rpm	WS m min <sup>-1</sup>	DDR	SST	Tenacity cN tex <sup>-1</sup>	Elongation %	Modulus cN tex <sup>-1</sup>	(W <sub>1/2</sub> ) <sup>-1</sup> degree	$\Delta n \times 1000$
1	0.35	17.7	230	3	400	444	A	16.1 (0.7)	574 (22)	44.5 (1.3)	1.14	27.2
2	0.35	17.7	230	12	100	29	C	5.0 (0.8)	1594 (114)	15.0 (1.0)	0.35	3.4
3	0.35	17.7	260	3	100	111	B	7.6 (0.6)	1000 (45)	13.9 (0.4)	0.35	12.2
4	0.35	17.7	260	12	400	114	B	10.6 (0.4)	690 (20)	19.1 (2.0)	0.36	10.3
5	0.35	22.4	230	3	100	111	B	8.2 (0.2)	790 (20)	27.1 (1.7)	1.02	10.4
6	0.35	22.4	230	12	400	114	B	9.5 (0.4)	778 (27)	38.4 (2.0)	1.33	9.8
7	0.35	22.4	260	3	400	444	A	12.1 (0.6)	516 (29)	38.8 (1.7)	1.24	32.5
8	0.35	22.4	260	12	100	29	C	5.1 (0.1)	1716 (122)	17.4 (1.3)	0.36	3.3
9	0.40	17.7	230	3	100	143	B	10.4 (0.7)	748 (21)	16.6 (1.8)	0.34	7.7
10	0.40	17.7	230	12	400	148	B	12.9 (0.5)	603 (51)	23.9 (2.0)	0.34	10.2
11	0.40	17.7	260	3	400	571	A	17.5 (1.0)	342 (21)	32.2 (0.7)	0.49	32.2
12	0.40	17.7	260	12	100	37	C	4.6 (0.6)	1748 (85)	17.8 (0.6)	0.36	2.7
13	0.40	22.4	230	3	400	571	A	12.7 (0.2)	514 (10)	46.4 (0.7)	1.49	31.7
14	0.40	22.4	230	12	100	37	C	5.5 (0.1)	1504 (65)	17.4 (0.6)	0.90	3.8
15	0.40	22.4	260	3	100	143	B	7.5 (0.8)	812 (76)	17.2 (0.9)	0.50	10.3
16	0.40	22.4	260	12	400	148	B	8.9 (0.4)	728 (37)	31.8 (2.0)	1.01	11.6

\* See Table I for the abbreviations of the control factors. DDR represents draw-down ratio, SST stress-strain type, (W<sub>1/2</sub>)<sup>-1</sup> crystallographic order, and  $\Delta n$  birefringence. The data in brackets are the standard deviation of five repeated measurements.

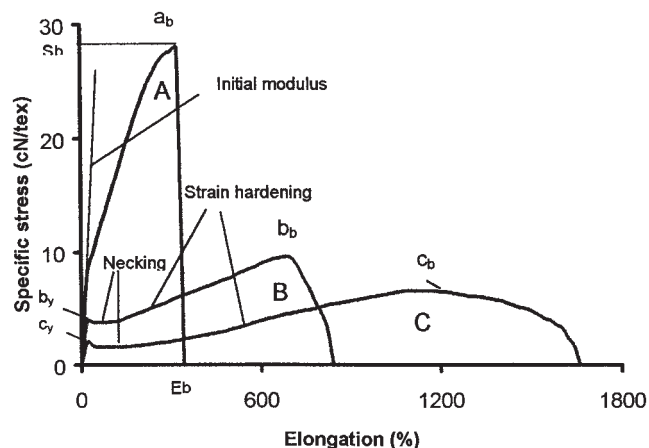


**Figure 2** Typical stress-strain curves of PP fibers. Curve A:  $a_b$  –breaking point,  $S_b$  –tenacity,  $E_b$  –elongation to break. Curves B and C:  $b_y$  and  $c_y$  –yield points,  $b_b$  and  $c_b$  –breaking points.

## RESULTS

### Deformation behavior at a constant stretching rate

The stress-strain curves obtained for our PP filaments present varying features, which can be broadly represented by curves A, B, and C, respectively, illustrated schematically in Figure 2. Curve A represents homogeneous deformation,<sup>3</sup> and curves B and C represent nonhomogeneous deformation. Curve C presents a weaker feature than curve B, with a lower yield stress (the stress at the yield point), lower tenacity, and greater elongation. In the case of homogeneous deformation, a steady increase in tensile force is required for further stretching beyond the initial linear region below about  $10 \text{ cN tex}^{-1}$  in curve A, until the breaking point,  $a_b$ , is reached. The specific stress and elongation at the breaking point afford the parameters,  $S_b$ , and elongation at break,  $E_b$ , which are commonly used to characterize filament strength and longitudinal deformation capacity, respectively. At the breaking point,  $a_b$ , the tensile force declines sharply to zero, associated with the complete breaking of all the filaments.

By contrast, nonhomogeneous deformation is characterized by a yield point ( $b_y$  and  $c_y$  in curves B and C, respectively). On reaching the yield point, filament diameter is reduced sharply and necking begins. During necking propagation, the filaments are elongated under an essentially constant tensile force. After completion of the necking process, further stretching requires increased tensile force again, until the breaking point ( $b_b$  and  $c_b$  in curves B and C, respectively) is reached. The breaking process of the filaments has been found to be more gradual compared with filaments that deform homogeneously. Indeed, the nonhomogeneously deforming filaments exhibit less strength and higher elongation to break than the homogeneously deforming filaments.

The stress-strain curves of all the as-spun PP samples have been classified into three groups, as listed in Table II under the heading SST (stress-strain types), the three groups being represented by the letters A, B, and C, respectively, corresponding to the three typical curves in Figure 2. It can be seen clearly from Table II that the types of stress-strain curve observed in the original series are completely reproduced in the duplicate series. Further, the classification is closely correlated to the DDR data: type A curves were obtained for high DDR ( $\geq 444$ ), type B for medium DDR (in the range 111–148), and type C for low DDR ( $\leq 37$ ). Therefore, draw-down ratio appears to exert a strong influence on the stress-strain behavior.

### Effects of spinning factors

From the stress-strain curves, values for tenacity, elongation to break, and specific secant modulus have been obtained for all 32 samples, 16 from the original series and 16 from the duplicate series. The data for the three mechanical properties, as responses to the process control factors, are listed in Table II. These data were analyzed using effects plots, ANOVA, and interaction plots.

Figure 3 shows the effects plots<sup>11</sup> for the mechanical properties of the two series. In such effects plots, the response values (on the y-axis) are plotted as a function of factor levels for each factor displayed on the x-axis, where the capital letters represent the individual processing factors and a block factor, and the lower case letters represent interaction factors. The block factor allows for the separation of the experiments into two days. It is clear that in the original series of trials (Fig. 3a), filament tenacity is significantly influenced by three main factors: winding speed, WS, metering pump speed, MPS, and the melt flow index, MFI. In addition, two interactions in columns **b** and **h** are relatively prominent. In the duplicate series (Fig. 3b), the main factors, WS and MPS, show similar prominence, but the effects of MFI and the interactions in columns **b** and **h** appear somewhat less prominent compared with those in the original series. Elongation to break (Figs. 3c and 3d) is significantly influenced by two main factors, WS and MPS, and one interaction in column **b**. The results from the original (Fig. 3c) and duplicate (Fig. 3d) series are very similar. In contrast, modulus (Fig. 3e) is markedly influenced by a number of factors, including four main factors: WS, MPS, MFI, and ST, and one interaction in column **b**. These results are reproduced in the duplicate series (Fig. 3f).

It is interesting to note that all three responses are markedly influenced by the main factors, WS and MPS. Tenacity and modulus are affected in the same direction, and elongation is affected in the opposite direction. Thus, a high level of WS and a low level of MPS result in an increase in tenacity and specific

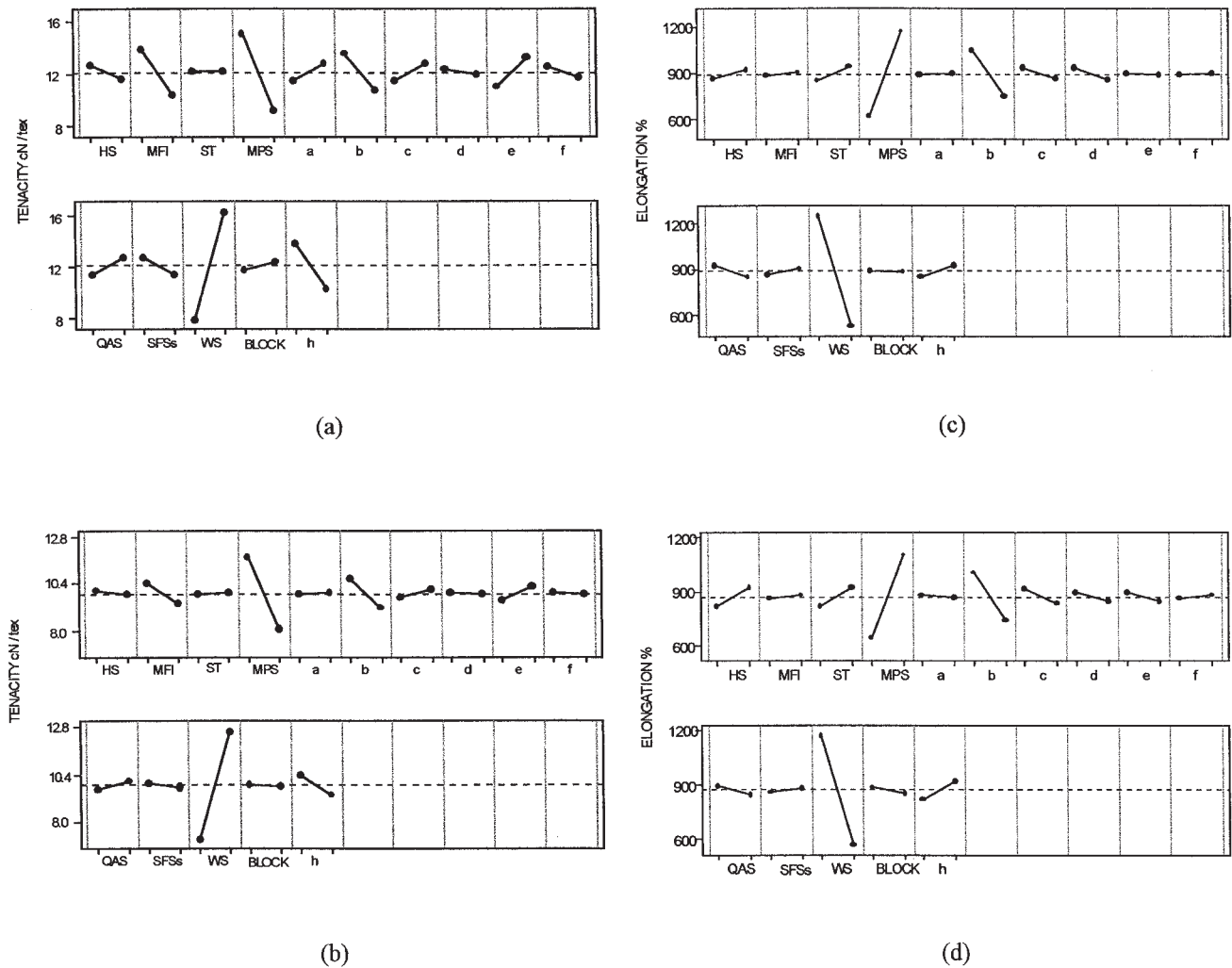


**Figure 3** Effects plots of tenacity (a and b), elongation to break (c and d), and specific secant modulus (e and f) for the original (a, c, and e) and the duplicate (b, d, and f) series of trials.

secant modulus, but a reduction in elongation to break. An increase in elongation requires a low level of WS in combination with a high level of MPS. Although in some cases the standard deviations of the response data (Table II) are appreciable, the same conclusions are reached separately from the two sets of data. These effects are consistent with the qualitative, direct observation of the types of stress-strain curves, which are decisively influenced by DDR (as shown in Table II). Another interesting point is the general presence of interaction effects, which are discussed below. In addition, the block effects, assigned to column BLOCK in Figure 3, are not significant for any of the three mechanical properties in the original and duplicate series. Thus, the separation of the experimental trials into two days did not contribute any significant effects. Further analysis through Daniel's plots leads to essentially the same conclusions.<sup>16</sup>

Table IV shows the results of ANOVA. These results reveal that WS and MPS, for which the probability  $P$  is very small indeed for all three tensile properties studied,

are highly significant statistically at the commonly used level of risk,  $\alpha = 0.05$ . The effect of MFI is significant for tenacity ( $P = 0.025$ – $0.031$ ) and specific secant modulus ( $P = 0.003$ – $0.018$ ), but not significant for elongation to break ( $P = 0.609$ – $0.793$ ). The effect of ST is significant for modulus ( $P = 0.008$ – $0.026$ ), but not significant for tenacity ( $P = 0.771$ – $0.985$ ) and apparently not significant for elongation ( $P = 0.052$ – $0.085$ ). The interaction effect in column **b** is significant for tenacity in the duplicate series, and for elongation and modulus in both series. The interaction effect in column **h** is significant for tenacity in both series, but for elongation only in the original series. The main effects from HS, QAS, and SFS<sub>2</sub> are not significant for any of the three mechanical properties. Overall, the ANOVA results are consistent with those from the effects plots and Daniel's plots.<sup>16</sup>

#### Evaluation of interaction effects

As described above, some discrepancy between the results from the original and duplicate series has been

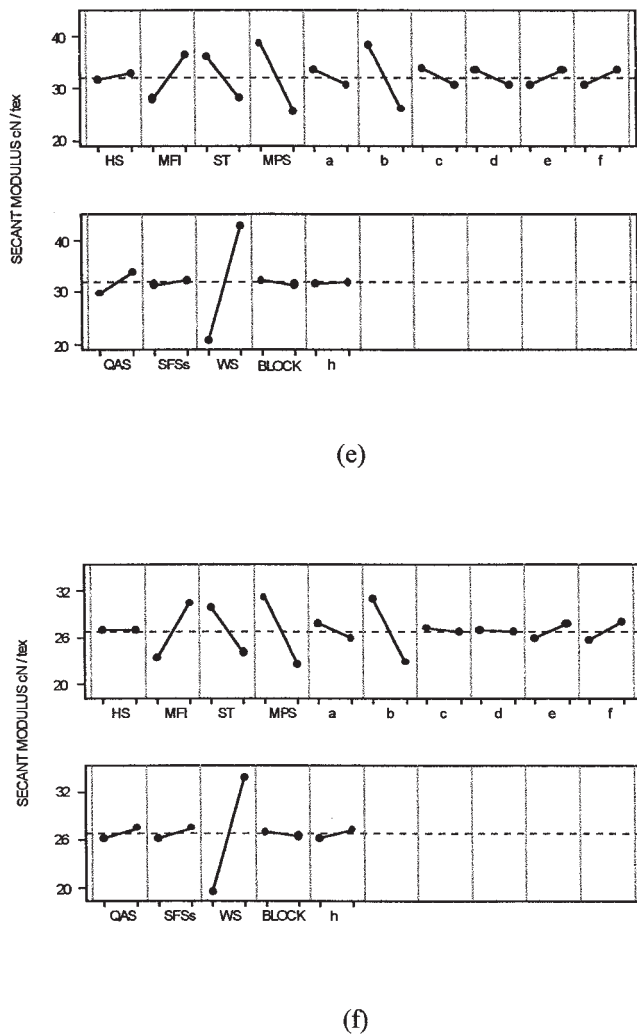


Figure 3 (Continued from the previous page)

observed concerning the statistical significance of some factor effects. Further, the exact source of interaction effects cannot be identified because of the limitation of the experimental design itself. Therefore, a third, confirmatory series of spinning experiments based on the results of the first two series has been carried out under a new design to resolve these indeterminate cases. In the new design, a higher resolution (level V) has been used, in which the two-factor interactions can all be individually identified.<sup>14</sup> To achieve the higher resolution, the factors QAS and SFS<sub>s</sub> were omitted. Table III lists the experimental array and the results obtained, together with the DDR data, SST observed, degree of crystallographic order,  $(W_{1/2})^{-1}$ , and birefringence data,  $\Delta n$ . The significance of  $(W_{1/2})^{-1}$  and  $\Delta n$  has been discussed in a previous paper.<sup>11</sup> The effects plots are shown in Figure 4. The ANOVA results for both main and interaction effects can be seen in Table V.

From the results of the third series, the following points can be made. First, the two main factors, MPS and WS, present highly significant effects on all three

mechanical properties. The dominant influence of these two factors, as revealed in the original and duplicate series, is thus confirmed. Accordingly, DDR as a function of these two factors does indeed exert a decisive influence on the tensile behavior of the as-spun PP fibers, as identified in the original and duplicate series: high values of DDR ( $\geq 444$ ) result in stress-strain curves of type A without exception, medium DDR (111–148) type B, and low DDR ( $\leq 37$ ) type C. Second, the effect of MFI on tenacity and specific secant modulus is also highly significant ( $P = 0.003$  and  $0.016$ , respectively), but its effect on elongation to break is not significant ( $P = 0.869$ ). The effect of ST on elongation is not significant ( $P = 0.233$ ), nor is its effect on tenacity ( $P = 0.119$ ). Its effect on modulus, however, does appear significant ( $P = 0.041$ ). The only remaining effect, HS, is not significant for any of the mechanical properties, in agreement with the results from the first two series. Third, the series has confirmed the existence of significant interaction effects and identified the exact sources. Among all ten two-factor interactions involved in the design, MPS\*WS is significant for elongation and modulus, and MFI\*WS for tenacity.

The effect of MPS\*WS on tenacity is intriguing. In the third series of experimental trials, the P value (0.437) suggests no statistical significance, whereas the P values from the original (0.069) and duplicate (0.004) series appear to show marginal lack of significance and high significance, respectively. The relatively big differences in P values from the three series may arise from random error, or Type II error.<sup>17</sup> (No human error was involved in data entry and analysis, which have been thoroughly checked.) It may also indicate a complex interaction effect of the two factors on the tenacity of as-spun PP fibers and, therefore, a definite conclusion cannot be reached.

**The directions of the significant interaction effects**

Figure 5 displays the surface plots of the three significant interaction effects to determine their directions. As can be seen from the figure, a surface plot is a three-dimensional representation of the response (the z dimension) as a function of the various combinations of the interacting main factors (the x and y dimensions). If an interaction between the main factors involved is absent, the surface of the plot is a plane. Significant interaction is manifest in the twist of the surface.<sup>13</sup> It is evident from the figure that high tenacity is associated with a low level of MFI and a high level of WS (Fig. 5a); high elongation to break with a high level of MPS and a low level of WS (Fig. 5b); and high specific secant modulus with a low level of MPS and a high level of WS (Fig. 5c). Therefore, increase in these responses is realized when the factors are altered in these directions, and *vice versa*. The directions of all three interaction effects are the same as those pre-

TABLE IV  
ANOVA Results for Tensile Properties\*

Source	DF		SS		MS		P	
	(a)	(b)	(a)	(b)	(a)	(b)	(a)	(b)
<u>Tenacity</u>								
HS	1	1	5.06	0.09	5.06	0.09	0.416	0.663
MFI	1	1	51.84	3.80	51.84	3.80	0.031	0.025
ST	1	1	0.00	0.04	0.00	0.04	0.985	0.771
MPS	1	1	146.41	56.25	146.41	56.25	0.003	0.000
QAS	1	1	7.84	0.42	7.84	0.42	0.319	0.360
SFS <sub>s</sub>	1	1	6.50	0.20	6.50	0.20	0.361	0.518
WS	1	1	278.89	118.81	278.89	118.81	0.001	0.000
b	1	1	32.49	9.00	32.49	9.00	0.069	0.004
h	1	1	49.00	3.42	49.00	3.42	0.035	0.030
Error	6	6	39.84	2.58	6.64	0.43		
Total	15	15	617.88	194.62				
<u>Elongation</u>								
HS	1	1	22052	41923	22052	41923	0.076	0.079
MFI	1	1	361	2730	361	2730	0.793	0.609
ST	1	1	28056	39900	28056	39900	0.052	0.085
MPS	1	1	1262252	874693	1262252	874693	0.000	0.000
QAS	1	1	16641	10558	16641	10558	0.112	0.329
SFS <sub>s</sub>	1	1	2704	2889	2704	2889	0.481	0.599
WS	1	1	2159430	1463495	2159430	1463495	0.000	0.000
b	1	1	390000	304428	390000	304428	0.000	0.001
h	1	1	32041	40502	32041	40502	0.042	0.083
Error	6	6	28822	56168	4804	9361		
Total	15	15	3942360	2837284				
<u>Modulus</u>								
HS	1	1	6.8	0.0	6.8	0.0	0.647	0.974
MFI	1	1	306.2	204.5	306.2	204.5	0.018	0.003
ST	1	1	249.6	138.1	249.6	138.1	0.026	0.008
MPS	1	1	665.6	306.3	665.6	306.3	0.003	0.001
QAS	1	1	65.6	6.5	65.6	6.5	0.184	0.426
SFS <sub>s</sub>	1	1	5.3	6.3	5.3	6.3	0.685	0.435
WS	1	1	1936.0	843.9	1936.0	843.9	0.000	0.000
b	1	1	627.5	277.2	627.5	277.2	0.004	0.001
h	1	1	0.7	3.1	0.7	3.1	0.880	0.579
Error	6	6	174.7	53.5	29.1	8.9		
Total	15	15	4038.1	1839.3				

\* Data in columns (a) and (b) are from the original and duplicate series, respectively. DF - degrees of freedom; SS - sum of squares; MS - mean square; P - probability.

sented by the related parameters as main factors (see Fig. 4).

### Optimization models

Bringing together the results and analysis of the three series of spinning experiments, Table VI lists models that specify the main factors and interaction factors significantly influencing the mechanical properties, and indicates the directions of factor change for optimization of these mechanical responses. The models of the structural properties, crystallographic order  $(W_{1/2})^{-1}$  and birefringence  $\Delta n$ , obtained from our previous paper,<sup>11</sup> are also listed in Table VI, for the purpose of discussion below. Increase in tenacity would be achieved under conditions of low levels of MFI and MPS and a high level of WS; increase in elongation to break by a high level of MPS and a low level of WS; increase in specific secant modulus by high levels of

MFI and WS and low levels of ST and MPS. By contrast, reduction of the responses would be achieved when the factor levels are changed in the opposite directions. It should be noted that interactions, as well as main effects, are included in these models.

## DISCUSSION

### Stress-strain curves

Depending on the spinning conditions, particularly the extent of draw-down, as-spun filaments assume different microscopic structures. With little or no draw-down, a structure of agglomerated spherulites<sup>18,19</sup> is predominant. It is well established that individual spherulites comprise stacks of lamellae, composed of regularly folded chains,<sup>20</sup> along radial directions. Moreover, the lamellae are linked by amorphous regions of tie molecules,<sup>21</sup> which constitute a

significant proportion of their overall mass. Within the amorphous regions, attraction between polymer chains is weak because of their random orientation and the large mean distances between them. Fibers with such a structure exhibit low tenacity, low specific secant modulus, and high elongation to break, characterized by a low yield stress and necking during the

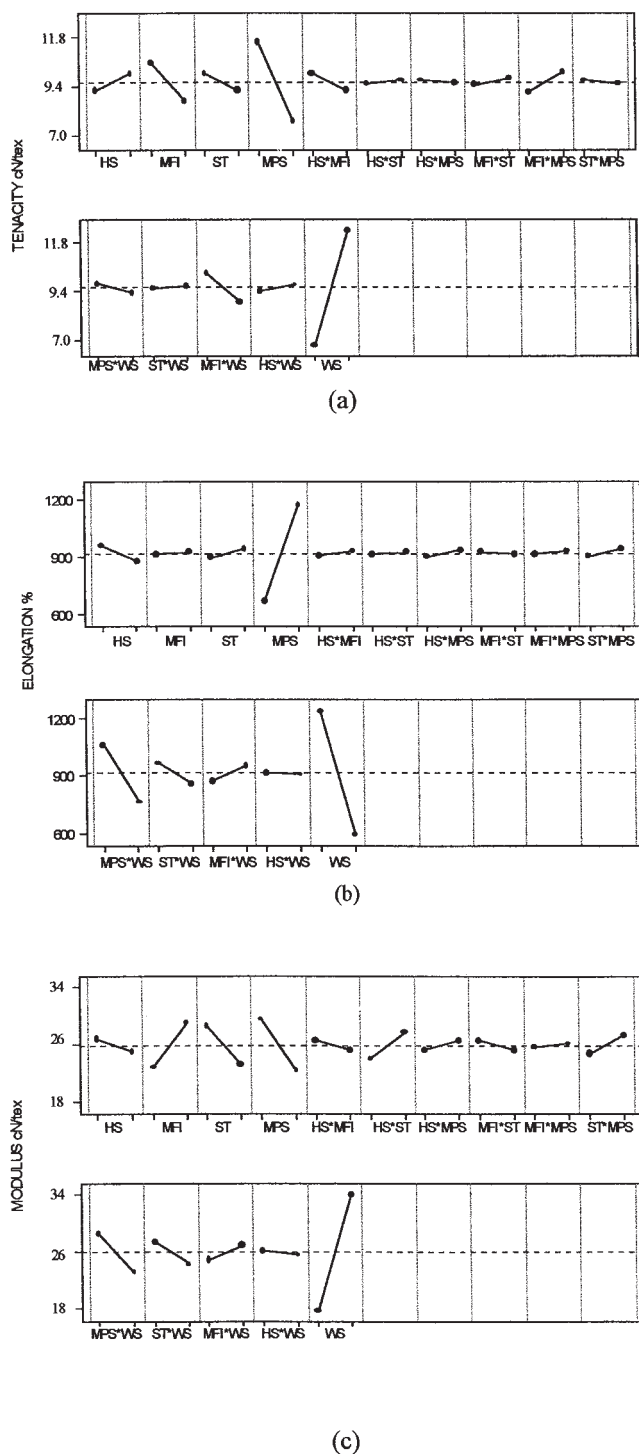


Figure 4 Effects plots of tenacity (a), elongation to break (b), and specific secant modulus (c) for the third series of trials.

TABLE V ANOVA Results for Tensile Properties of the Third Series\*

Source	DF	SS	MS	P
<u>Tenacity</u>				
HS	1	2.10	2.10	0.152
MFI	1	14.44	14.44	0.003
ST	1	2.56	2.56	0.119
MPS	1	56.25	56.25	0.000
WS	1	134.56	134.56	0.000
MFI*WS	1	9.92	9.92	0.009
MPS*WS	1	0.56	0.56	0.437
Error	8	6.72	0.84	
Total	15	227.12		
<u>Elongation</u>				
HS	1	27143	27143	0.093
MFI	1	218	218	0.869
ST	1	12488	12488	0.233
MPS	1	1032764	1032764	0.000
WS	1	1668618	1668618	0.000
MFI*WS	1	22127	22127	0.124
MPS*WS	1	347805	347805	0.000
Error	8	59939	7492	
Total	15	3171101		
<u>Modulus</u>				
HS	1	7.43	7.43	0.537
MFI	1	165.77	165.77	0.016
ST	1	105.58	105.58	0.041
MPS	1	195.30	195.30	0.011
WS	1	1100.58	1100.58	0.000
MFI*WS	1	24.75	24.75	0.272
MPS*WS	1	107.64	107.64	0.039
Error	8	142.51	17.81	
Total	15	1849.55		

stress-strain curve, as shown by curve C, and to a lesser extent by curve B in Figure 2. If draw-down is more pronounced, the spherulitic structure is altered progressively towards a microfibrillar structure,<sup>19,22</sup> comprising crystallites, amorphous regions of interfibrillar tie molecules connecting the adjacent crystallites, microfibrils, and extended noncrystalline regions of interfibrillar tie molecules connecting adjacent microfibrils.<sup>16,23</sup> In the microfibrillar structure, crystallinity is increased significantly, and both types of tie molecule are more extended and aligned compared with those in the spherulitic structure. The overall result is a significant reduction in the mean distance between polymer chains and a consequent increase in intermolecular attraction. As-spun fibers produced at higher draw-down assume structures closer to the interfibrillar structure and hence exhibit higher tenacity, higher specific secant modulus, and lower elongation to break. In the stress-strain curve, the yield point and necking are both absent, as shown by curve A in Figure 2.

Significant processing factors

The three series of results presented above have identified all the main factors and interaction factors that



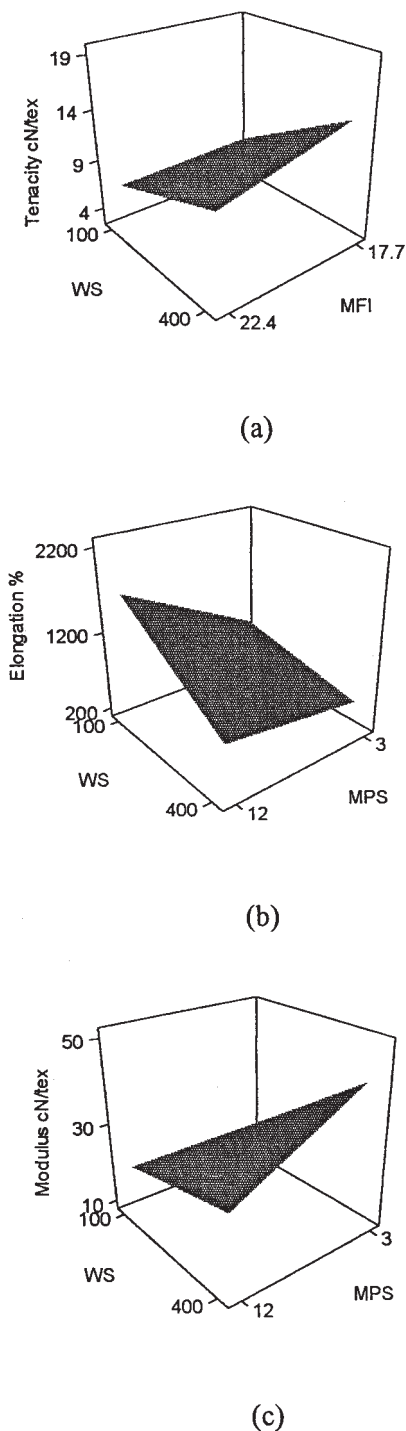


**Figure 5** Surface plots for tenacity (a), elongation to break (b), and specific secant modulus (c).

significantly affect tenacity, elongation to break, and specific secant modulus. The directions of factor change for optimizing these properties have also been determined. The concise statistical models summarizing these results (Table VI) enable as-spun PP fibers to be tailor-made for specific technical requirements. However, beyond the practical point of view of manufacturing, interesting questions still arise: why do

these particular factors significantly influence some or all of the mechanical properties, and what is the physicochemical basis for the results? These questions are important for improved understanding of the process-property relationship and for further quantitative modeling of the process.

This section of the paper attempts to resolve these questions in terms of the microscopic structure and the intermolecular forces governing the mechanical behavior of the PP fibers. It is noteworthy (Table VI) that elongation to break and overall PP chain orientation, as expressed by  $\Delta n$ , are significantly influenced by identical factors, albeit in opposite directions. Moreover, the individual processing parameters significantly affecting specific secant modulus are the same as those influencing crystallographic order,  $(W_{1/2})^{-1}$ . No such direct relation with structural properties is, however, evident for tenacity.

### Filament tenacity

Filament tenacity is significantly influenced by three main processing factors, WS, MPS, and MFI, and by one interaction, MFI\*WS. As noted above, an increase in WS and a decrease in MPS both serve to increase DDR. An increase in DDR facilitates strain-induced crystallization, enhances the orientation of crystallites and microfibrils, promotes extension and alignment of tie molecules, and thus enhances overall orientation, as revealed by the birefringence results<sup>11</sup> (Table III). The extension and alignment of tie molecules reduce intermolecular distances and hence tend to augment the overall strength of interaction between adjacent PP chains. Filament tenacity is, therefore, increased.

The significant influence of melt flow index, MFI, on fiber tenacity draws attention to the importance of the grade of PP used. Although MFI is dependent on several factors, including weight-average molar mass, molar mass distributions, and any impurities present, it is likely that, of the two grades used in this work, the grade with the lower MFI possesses the longer polymer chains.<sup>3</sup> Thus, an increase in average chain length, which is associated with a reduced melt flow index, MFI (L), increases the population of tie molecules,<sup>3,24</sup> thereby promoting cohesion between the crystallites and microfibrils present in the filaments. The increased average length of molecular chains also increases spin-line stress and hence facilitates the extension and orientation of the structural elements comprising each filament,<sup>25-27</sup> with a consequent increase in tenacity (Table VI). On the other hand, long molecular chains are more inclined to entangle with one another and are difficult to crystallize, a feature that is detrimental to tensile strength.<sup>28</sup> This effect can be countered substantially by an increased winding speed WS (H), which intensifies stretching and hence alignment of molecular chains. Therefore, the interac-

**TABLE VI**  
**Summary of the Major Models for PP Spinning Process**

Physical characteristics	Significant factors		P value	Statistical models*
	Main factors	Interaction factors		
Tenacity	WS		0.000	WS (H)
	MPS		0.000	MPS (L)
	MFI		0.003	MFI (L)
		MFI*WS	0.009	
Elongation	WS		0.000	WS (L)
	MPS		0.000	MPS (H)
		MPS*WS	0.000	
Modulus	WS		0.000	WS (H)
	MPS		0.001	MPS (L)
	MFI		0.003	MFI (H)
	ST		0.026	ST (L)
		MPS*WS	0.001	
$(W_{1/2})^{-1}$	WS		0.002	WS (H)
	MPS		0.038	MPS (L)
	MFI		0.000	MFI (H)
	ST		0.009	ST (L)
$\Delta n$	WS		0.000	WS (H)
	MPS		0.000	MPS (L)
		MPS*WS	0.000	

\* Letters H and L in brackets represent high and low levels of the control parameters, respectively, for increasing the responses.

tion MFI (L)\*WS (H) will lead to an increase in tenacity.

### Elongation to break

The opposite effect of WS and MPS on elongation to break compared with that on tenacity (Table VI) can also be accounted for by the increased structural alignment and intermolecular attraction achieved through an increased DDR. A high degree of draw-down results in a high degree of extension of molecular chains and orientation of other structural units,<sup>7</sup> which enhances filament tenacity but reduces the capacity for further longitudinal deformation during testing. Conversely, a reduction in DDR decreases the overall orientation and increases the elongation to break. The interaction, MPS\*WS, acts in the same directions as the two main factors individually and can be explained in the same way.

### Specific secant modulus

The effects of processing factors on specific secant modulus can, we suggest, be largely rationalized in terms of the degree of crystallographic order,<sup>6</sup> as determined by  $(W_{1/2})^{-1}$ . In a crystallized state, the molecular chains are held tightly in the lattice and any relative movement beyond that allowed by equilibrium vibration is difficult owing to significant lattice

energy. Further, the movement of molecular chains immediately surrounding the crystalline lamellae in a spherulitic structure or the crystallites in a microfibrillar structure is more restricted compared with those in a completely amorphous surrounding; many of these molecules are partly incorporated into the lamellae or crystallites and are held more closely to one another. Therefore, an increase in the crystallographic order contributes most effectively to filament stiffness, as measured by specific secant modulus. This accounts for the observation that the same factors, WS, MPS, MFI, and ST, which significantly influence specific secant modulus also influence crystallographic order in the same directions (Table VI). Specifically, an increase in DDR, resulting from a combination of increased winding speed WS (H) and decreased metering pump speed MPS (L), promotes "orientation induced crystallization," and hence an increase in modulus. Shorter molecular chains, associated with a high level of MFI (H), are easier to stretch, align, and pack into a crystal lattice owing to a smaller degree of entanglement, and are favorable for crystallization.<sup>3</sup> A reduced spinning temperature ST (L) lowers the internal energy of the system, which lessens the thermal motion of the molecular chains. This, in turn, facilitates polymer crystallization and hence also results in an increase in specific secant modulus and crystallographic order.

It is noteworthy (Table VI) that the interaction MPS\*WS appears significant for specific secant modulus but not for crystallographic order,  $(W_{1/2})^{-1}$ . However, it can also be noted that the effect from MPS itself, as a main factor, appears decidedly more significant on modulus ( $P \leq 0.001$ ) than on crystallographic order ( $P = 0.038$ ) at a level of confidence,  $\alpha = 0.05$ . Factors with weaker main effects are normally less likely to be involved in significant interaction effects.

## CONCLUSIONS

The tenacity, elongation to break, and specific secant modulus of as-spun PP filaments have been studied as functions of spinning conditions using a comprehensive statistical approach. The approach comprises a one-step overall design of the experiment and systematic statistical analysis of the results, leading to concise models for optimization. The property-processing relationships established have been rationalized through correlation with microscopic structure, in terms of crystallographic order and overall orientation, which have been described previously.<sup>11</sup> Results from the three series of experiments serve to confirm that the structure and properties are decisively influenced by draw-down ratio (DDR) of the spinning process, reflecting the effects from winding speed and metering pump speed as main factors and, importantly, also through their interaction. Specifically, tenacity is influenced by DDR in the same way as overall orientation, but is dependent too on the grade of PP raw material. Specific secant modulus and crystallographic order are affected in the same manner by melt flow index and spinning temperature, in addition to DDR. Using the same experimental conditions, elongation to break varies in the opposite direction compared with tenacity. Significant interaction effects are generally present for all three responses.

An increase in the responses can be achieved under conditions of WS (H), MPS (L), and MFI (L) for tenacity; WS (L) and MPS (H) for elongation to break; and WS (H), MPS (L), MFI (H), and ST (L) for specific secant modulus. A reduction in the responses is achieved when the control parameters are changed in the opposite directions.

The results clearly demonstrate that the statistical approach is well suited to the development of synthetic fiber process technology, efficiently leading to more reliable and accurate results based on a small number of experiments. The systematic processing-structure-property correlation established through the statistical approach offers a real possibility of controlling mechanical properties of fiber filaments through modification of microscopic structure via process technology. Wide use of the statistical approach in fiber engineering would hence be beneficial.

The authors thank Heriot-Watt University for financial support to RY; Borealis and Finapro for supplying the PP raw materials; Mr. T. Storer, Dr. R. B. Hammond, and Dr. A. Korabinski for technical support and discussions; and Mr. G. Loveridge at Becton Dickinson for the measurement of the MFI data of the raw materials.

## References

1. Anon., *Chem Fibres Int* 1998, 48, 363.
2. Schmenk, B.; Miez-Meyer, R.; Steffens, M.; Wulfhorst, B.; Gleixner, G. *Chem Fibres Int* 2000, 50, 233.
3. Ahmed, M. *Polypropylene Fibers—Science and Technology*; Elsevier: Amsterdam, Oxford, and New York, 1982.
4. Parys, M. V. *Chem Fibres Int* 1998, 48, 317.
5. Backhouse, P. G.; Fotheringham, A. F.; Allan, G. *Using Experimental Design and Neural Network Techniques to Optimise Multi-Filament Polypropylene Yarns—A Case Study*; Proceedings of the World Textile Congress, Huddersfield, UK, 1996.
6. Yang, R. D.; Mather, R. R.; Fotheringham, A. F. *Int Polym Processing* 1999, 14, 60.
7. Mather, R. R.; Fotheringham, A. F.; Yang, R. D. *Factorial Experimental Design in the Processing of Polypropylene Fibres*; Proceedings of the Textile Institute Conference on Fibre Science/Dyeing and Finishing, Prestbury, Cheshire, UK, 1999.
8. Yang, R. D.; Mather, R. R.; Fotheringham, A. F. *J Mater Sci* 2001, 36, 3097.
9. Yang, R. D.; Mather, R. R.; Fotheringham, A. F. *Modelling the Drawing of Polypropylene Fibres: Control Factors and their Interactions*; Proceedings of the World Congress on PP in Textiles, Huddersfield, UK, 2000.
10. Zanetti, R.; Celotti, G.; Fichera, A.; Grancesconi, R. *Die Makromolekulare Chemie* 1969, 128, 137.
11. Yang, R. D.; Mather, R. R.; Fotheringham, A. F. *J Appl Polym Sci*, 2004, 93, 568.
12. Lochner, R. H.; Matar, J. E. *Designing for Quality*; Chapman and Hall: London, 1989.
13. Montgomery, D. C. *Design and Analysis of Experiments*, 4<sup>th</sup> ed.; John Wiley & Sons: New York, 1997.
14. Logothetis, N.; Wynn, H. P. *Quality through Design*; Clarendon Press: Oxford, 1989.
15. Ross, P. J. *Taguchi Techniques for Quality Engineering*; McGraw-Hill: New York, 1998.
16. Yang, R. D. Ph.D. Thesis, Heriot-Watt University, 2000.
17. Hayslett, H. T. *Statistics Made Simple*; Butterworth-Heinemann: Oxford, UK, 1981; p. 103.
18. Samuels, R. J. *Structured Polymer Properties*; John Wiley & Sons: New York, 1974.
19. Lee, Y. W.; Li, J. X. *J Appl Polym Sci* 1993, 48, 2213.
20. Lindenmeyer, P. H. *J Polym Sci, Part C* 1967, 20, 145.
21. Samuels, R. J. *J Macromol Sci-Phys* 1970, B4, 3,701.
22. Risnes, O. K.; Mather, R. R.; Neville, A. *Polymer* 2003, 44, 89.
23. Prevorsek, D. C.; Tirpak, G. A.; Harget, P. J.; Reimschuessel, A. C. *J Macromolsci-Phys B9* 1974, 4, 733.
24. Peterlin, A. *J Mater Sci* 1971, 6, 490.
25. Spruiell, J. E.; White, J. L. *Appl Polym Symp* 1975, 27, 121.
26. Ziabicki, A.; Kawai, H. *High-Speed Fibre Spinning, Part III Development of Fibre Structure and Properties*; John Wiley & Sons: New York, 1985.
27. Nadella, H.; Henson, H. M.; Spruiell, J. E.; White, J. L. *J Appl Polym Sci* 1977, 21, 3003.
28. Cowie, J. M. G. *Polymers: Chemistry and Physics of Modern Materials*; Chapman and Hall: New York, 1991.